ACADEMIC PRESS

Available online at www.sciencedirect.com

SCIENCE DIRECT®

Journal of Sound and Vibration 265 (2003) 109–121

JOURNAL OF SOUND AND VIBRATION

www.elsevier.com/locate/jsvi

Failures in the discrete models for flow duct with perforations: an experimental investigation

Y. Aurégan*, M. Leroux

Laboratoire d'Acoustique de l'Université du Maine, UMR CNRS 6613, Av. O Messiaen, 72085 Le Mans cedex 9, France

Received 11 March 2002; accepted 3 July 2002

Abstract

Acoustical experiments have been performed at low frequencies on perforated tubes with a back cavity by means of the "2 sources method" and are compared to classical models. The four elements of the transfer matrix of the device are measured with flow. The classical lumped model relates the sound pressure and the axial velocity on both sides of the lined region. Since this model fails, a new empirical model has been proposed to take into account the experimental data. The new transfer matrix of the measured device is calculated and the results fit surprisingly well with the experiments. It is therefore possible to make a segmentation model of the aeroacoustical behaviour of a perforated tube with a partitioned chamber.

1. Introduction

Perforated plates or tubes with back cavities are widely used to attenuate sound. Two different approaches can be used to model the perforations. In the continuous approach, the perforated plate is seen as a continuous media, and the local pressure difference on both sides of the plate is linearly dependent on the local transverse velocity passing through the plate. This approach can be found at low frequencies in engine exhaust systems (see for example Refs. [1–3]), but also at higher frequencies in aircraft engine liners (see for example Ref. [4]). Another approach is the discrete approach, known as the segmentation model [5]. In this approach each row of perforations is considered separately. This kind of modelling has proved to be useful when no flow is present [6,7]. The segmentation model has also been used with flow [5,8,9], but there is no experimental evidence of the accuracy of the model in this case.

*Corresponding author. Tel.: +33-2-43-833509; fax: +33-2-43-833520.
E-mail address: yves.auregan@univ-lemans.fr (Y. Aurégan).

0022-460X/03/$ - see front matter
doi:10.1016/S0022-460X(02)01442-6

This paper examines experimentally the underlying assumptions of the segmentation model with flow. The comparison between the experimental and theoretical results shows that the current model does not correctly describe the effect of mean flow.

The experimental apparatus is described in Section 2. The devices investigated are perforated tubes surrounded by a partitioned chamber. In the low frequencies limit (the reduced frequency range ka is 0.08–0.3, with a the radius of the tube and k the wavenumber), this lined duct is described by a 2×2 transfer matrix, connecting two acoustical variables at the inlet to two acoustical variables at the outlet. Measurements of the four elements of this matrix are performed with the experimental apparatus.

The duct investigated reacts locally. Thus, using the segmentation model, the four matrix elements as a function of the perforation impedance are known. Therefore, three compatibility relations exist independently of the value of the perforation impedance. Section 3 shows that these three relations are not experimentally verified and an empirically modified segmentation model is given.

2. Experiments

2.1. Measuring technique

The aim of the experimental apparatus is to measure the transfer matrix or the scattering matrix of an element in the presence of a mean flow. The scattering matrix [S] relates the scattered pressure amplitudes p_1^- and p_2^+ to the incident pressure amplitudes p_1^+ and p_2^- as follows:

$$\begin{pmatrix} p_1^- \\ p_2^+ \end{pmatrix} = [\mathbf{S}] \begin{pmatrix} p_1^+ \\ p_2^- \end{pmatrix} = \begin{bmatrix} R^+ & T^- \\ T^+ & R^- \end{bmatrix} \begin{pmatrix} p_1^+ \\ p_2^- \end{pmatrix}, \tag{1}$$

where T^+ and T^- are the anechoic transmission coefficients, R^+ and R^- are the anechoic reflection coefficients, and the subscripts $i = 1, 2$ indicate the inlet and the outlet, respectively (see Fig. 1). Åbom [10] reviews the ways of measuring these matrices.

The transfer matrix [T] is defined by

$$\begin{pmatrix} p_2 \\ u_2 \end{pmatrix} = [\mathbf{T}] \begin{pmatrix} p_1 \\ u_1 \end{pmatrix} = \begin{bmatrix} A & B \\ C & D \end{bmatrix} \begin{pmatrix} p_1 \\ u_1 \end{pmatrix}, \tag{2}$$

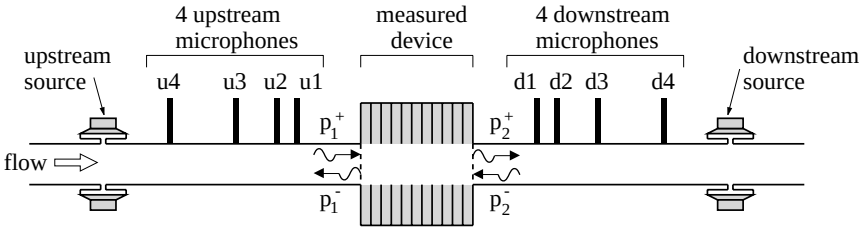

Fig. 1. General view of the experimental apparatus.

where $p_i = p_i^+ + p_i^-$ and $u_i = p_i^+ - p_i^-$ ($i = 1$ at the inlet and $i = 2$ at the outlet). The transfer matrix elements are found by

$$A = (T^+T^- + (1 - R^+)(1 + R^-))/2T^-,$$
$$B = (T^+T^- - (1 + R^+)(1 + R^-))/2T^-,$$
$$C = (T^+T^- - (1 - R^+)(1 - R^-))/2T^-,$$
$$D = (T^+T^- + (1 + R^+)(1 - R^-))/2T^-.$$

The method of measurement used in this paper is referred to as the "2 sources method". Experiments are carried out for two different states of the system. The first state is obtained by switching on the upstream source, while the downstream source is switched off, and the second state by switching on the downstream source, while the upstream source is switched off.

The scattering matrix is calculated from the two measurements using the following relation:

$$\begin{bmatrix} (p_1^-/p_1^+)^{\mathrm{I}} & (p_1^-/p_2^-)^{\mathrm{II}} \\ (p_2^+/p_1^+)^{\mathrm{I}} & (p_2^+/p_2^-)^{\mathrm{II}} \end{bmatrix} = [\mathbf{S}] \begin{bmatrix} 1 & (p_1^+/p_2^-)^{\mathrm{II}} \\ (p_2^-/p_1^+)^{\mathrm{I}} & 1 \end{bmatrix}, \tag{3}$$

where the superscripts indicate the measurement. This calculation is meaningful only if the two measurements are independent, i.e., if the determinant of the second right side matrix does not vanish: $(p_2^-/p_1^+)^{\mathrm{I}} \neq (p_1^+/p_2^-)^{\mathrm{II}}$.

The coefficients of the matrix in Eq. (3) are found from the transfer functions between the different microphones as follows:

$$(p_1^-/p_1^+)^{\mathrm{I}} = \frac{H_{u_j u_i}^{\mathrm{I}} \mathrm{e}^{-jk^+ x_{u_i}} - \mathrm{e}^{-jk^+ x_{u_j}}}{\mathrm{e}^{jk^- x_{u_i}} - H_{u_j u_i}^{\mathrm{I}} \mathrm{e}^{jk^- x_{u_j}}}, \tag{4}$$

where $H_{u_j u_i}^{\mathrm{I}}$ is the transfer function between the microphones u_j and u_i obtained in the measurement I, k^+ and k^- are the wavenumbers in the pipe in the direction of the flow and in the reverse direction, respectively, and x_{u_i} is the position of the microphone u_i relative to the inlet of the measured element. All the other matrix elements can be deduced the same way (see Ref. [11] for details). The key point here is that the wavenumbers k^+ and k^- have to be known in order to calculate the scattering matrix. The wavenumbers in the tube on both sides of the measured device are given by the quasilaminar theory of Ronneberger [12] corrected by the turbulence-acoustic boundary layer interaction at low frequency [13–15].

2.2. Experimental set-up

Two measuring pipes are fitted to the inlet and the outlet of the device being measured. The inner diameter of these steel pipes is $a = 30$ mm and their wall thickness is 4 mm. The pipes have a smooth inner wall with a roughness of less than 0.1 μm.

Four microphones (B&K 4136 and 2670 with Nexus 2690 amplifier) are used on each side of the measured device. The method of transfer functions is known [10] to give poor results when the wavelength λ is close to twice the distance between the microphones. The use of four microphones

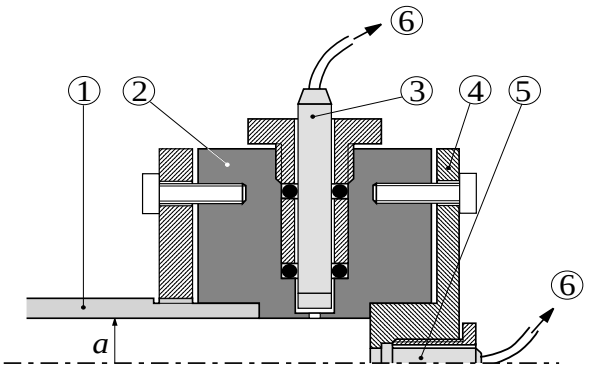

Fig. 2. Schematic view of the microphone setting. (1) Pipe, (2) microphone support, (3) B&K microphone, (4) calibration cap, (5) PCB pressure gauge, (6) to the analyzer.

avoids this problem. The distances between the microphones are $x_{u_1} - x_{u_2} = x_{d_2} - x_{d_1} = 0.1$ m, $x_{u_1} - x_{u_3} = x_{d_3} - x_{d_1} = 0.475$ m, and $x_{u_1} - x_{u_4} = x_{d_4} - x_{d_1} = 1.0715$ m. Calibration of the operating microphones involves a reference pressure gauge (PCB 116B) mounted flush in a cap (see Fig. 2).

The signal from the microphones is transferred to an HP 3565 data acquisition system. This system is used in the sine sweep mode and an average over 300 cycles is used at each frequency step. The HP 3565 system provides the output signal to drive the sources. Each source is composed of four loudspeakers specially chosen to generate a sound pressure level reaching 140 dB in the pipe over the frequency range 30–1000 Hz. To avoid standing waves, weakly reflective terminations are used on both sides of the measuring pipes.

The mean flow in the pipe comes from a compressor (Aerzen Delta blower GM10S) which can supply a flow rate up to 0.15 $m^3\ s^{-1}$. The air flow is cooled before measurement in an ITT Barton 7445 flowmeter. The temperature in the pipe is evaluated by means of two temperature sensors located on the wall, one on each side of the measured device the transfer matrix of which is to be determined. The use of four microphones gives rise to an overestimation of the data. A correction of the effects of the temperature on the wavenumbers is then applied.

2.3. Measured devices

Experiments were carried out on a partitioned chamber with a perforated tube (Fig. 3a). To obtain as local a reaction as possible, the back cavity (inner radius = 16 mm, outer radius $b = 50$ mm) is divided into N_c cells by $N_c - 1$ separating discs. These discs have a thickness of 0.5 mm and the distance between two discs is 7 mm.

The wall of the lined section consists of a copper tube of inner radius $a = 15$ mm and of thickness = 1 mm. The characteristics of the different devices used for the measurements are given in Table 1: N_c is the number of cells, L_c is the length of one cell, L_r is the distance between two rows of perforations, n_p is the number of perforations per row, and D is the diameter of the perforations (Figs. 3b and c).

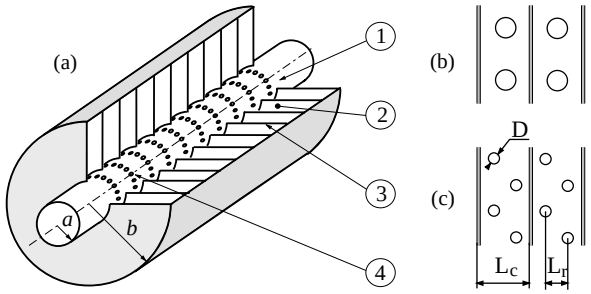

Fig. 3. (a) Schematic view of the partitioned chamber with perforated tube. (1) Perforated tube, (2) back cavity, (3) dividing disc, (4) row of perforations, (b) perforations for devices 1 and 2, (c) perforations for devices 3 and 4.

Table 1
Characteristics of the four devices used for the measurements

Device	N_c	L_c	L_r	n_p	D
1	10	7.5	7.5	12	3
2	6	7.5	7.5	12	3
3	10	7.5	3.25	24	1.5
4	6	7.5	3.25	24	1.5

The distances are in mm.

Thus, each cell is composed of a tube of length L_c coupled by one or two rows of perforations to a back cavity. The resonance frequency ($\sim$1100 Hz) of the cells is chosen to be outside of the frequency range being tested (30–1000 Hz) to avoid nonlinearities in the perforations.

The measured reflection and transmission coefficients of device 1 are plotted as a function of the frequency in Fig. 4. Without flow (dashed line), the chamber is exactly symmetric: $R^+ = R^-$ and reciprocal: $T^+ = T^-$. With flow (solid line), symmetry and reciprocity are broken. Similar observations are made for the other devices described in Table 1.

3. Segmentation model

3.1. Discrete model for perforation with flow

The segmentation model was developed by Sullivan [5] to analyze perforated mufflers. This model has been generalized by Kergomard et al. [6] without flow, and recently used by Dokumaci [9]. In this paper, the perforated tube is divided into segments containing only one cell.

In the tube the convected equations for mass and momentum are used. A lumped model is deduced from integrated mass and momentum equations for a perfect fluid in the perforations region. This lumped model relates the acoustical pressure and the axial velocity on both sides of the perforations. To our knowledge, this lumped model for perforation with flow has never been validated experimentally.

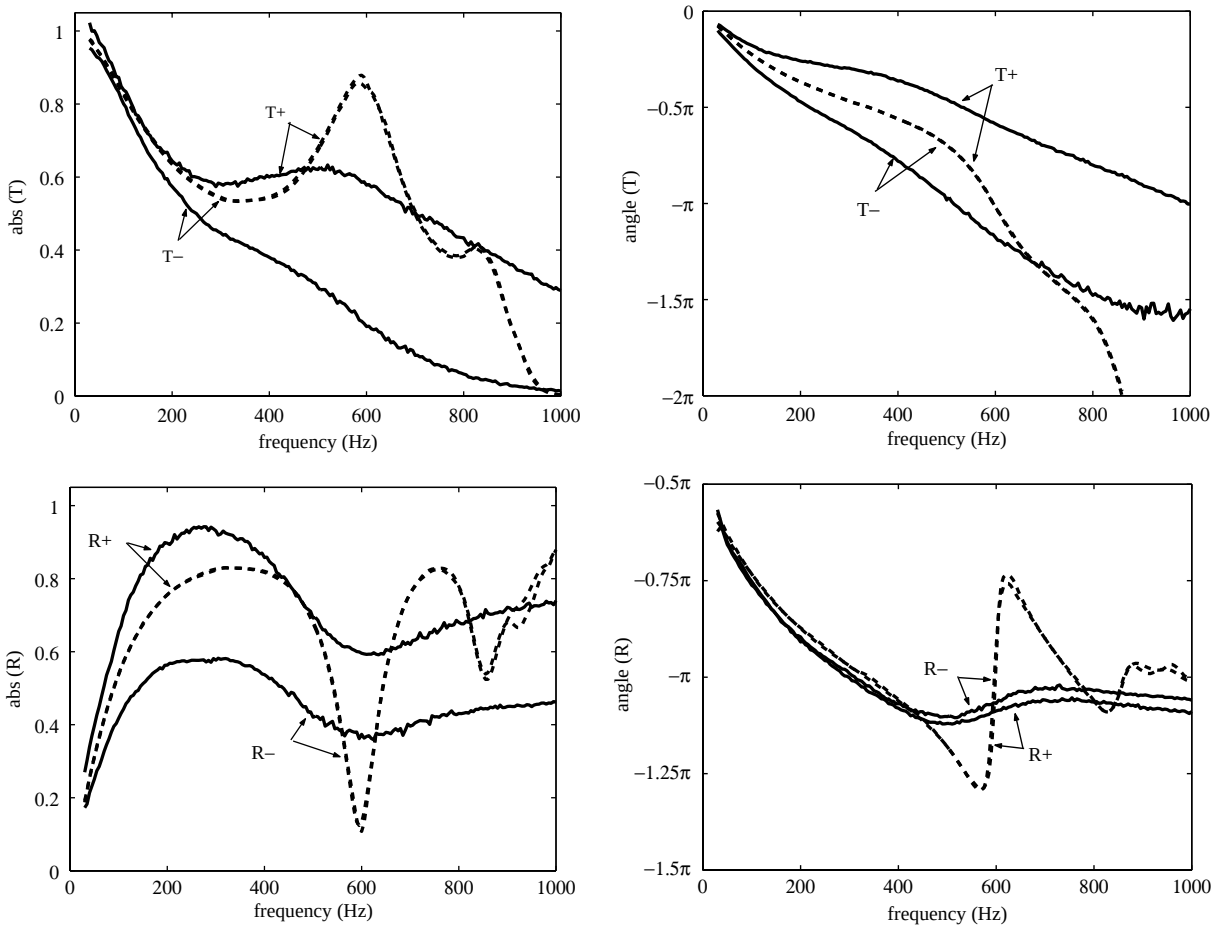

Fig. 4. Device 1: Reflection and transmission coefficients of the partitioned chamber with a perforated tube. – – –, $M = 0$; ——, $M = 0.143$.

From the experimental data on the partitioned chamber with a perforated tube, it is easy to find the transfer matrix of one cell because the system is assumed to be periodic. Then, the transfer matrix of one cell $[\mathbf{T}_c]$, relating pressure and velocity in section a and b (see Fig. 5), is deduced from the transfer matrix of the chamber $[\mathbf{T}]$ by

$$[\mathbf{T}_c] = [\mathbf{T}]^{1/N_c}, \tag{5}$$

where N_c is the number of cells. The transfer matrix of one cell may be written as follows:

$$[\mathbf{T}_c] = [\mathbf{T}_t][\mathbf{T}_p][\mathbf{T}_t], \tag{6}$$

where $[\mathbf{T}_t]$ is the classical transfer matrix of a tube of length $L_c/2$ with a uniform flow of Mach number M, and $[\mathbf{T}_p]$ is the transfer matrix of the perforations relating pressure and velocity in

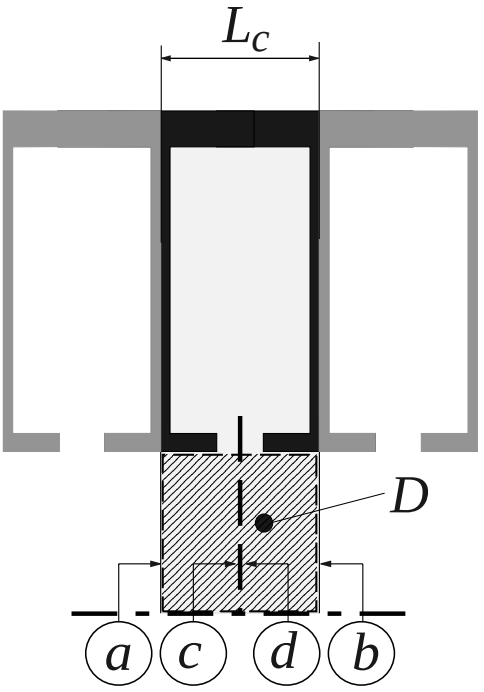

Fig. 5. Schematic view of one cell.

section c and d (see Fig. 5):

$$\begin{pmatrix} p_d \\ u_d \end{pmatrix} = [\mathbf{T}_p] \begin{pmatrix} p_c \\ u_c \end{pmatrix} = \begin{bmatrix} A_p & B_p \\ C_p & D_p \end{bmatrix} \begin{pmatrix} p_c \\ u_c \end{pmatrix}. \tag{7}$$

According to the lumped model of Sullivan [5,9], the reduced pressure and the reduced velocity (made dimensionless by $\rho_0 c_0^2$ and c_0, respectively) on both sides of the perforations are related by

$$p_d + Mu_d = p_c + Mu_c, \tag{8}$$

$$u_d + Mp_d = u_c + Mp_c + Y_s(p_c + Mu_c), \tag{9}$$

where Y_s is the reduced admittance of the perforations plus the back cavity. This is equivalent to

$$\begin{pmatrix} p_d \\ u_d \end{pmatrix} = \begin{bmatrix} 1 - Y_s M/(1-M^2) & -Y_s M^2/(1-M^2) \\ Y_s/(1-M^2) & 1 + Y_s M/(1-M^2) \end{bmatrix} \begin{pmatrix} p_c \\ u_c \end{pmatrix}. \tag{10}$$

Comparing Eqs. (7) and (10), the admittance used in the lumped model can be deduced from the measured coefficient C_p by $Y_s = (1-M^2)C_p$. Introducing this value in Eq. (10), the theoretical value of the transfer matrix is calculated using Eqs. (5) and (6).

Without flow, the agreement is perfect between the theoretical value of the transfer matrix obtained in this way and the experimental value.

With flow, this theoretical value of the scattering coefficients is compared in Fig. 6 to the experimental results for device 1. The agreement is poor. The most striking point is that the model

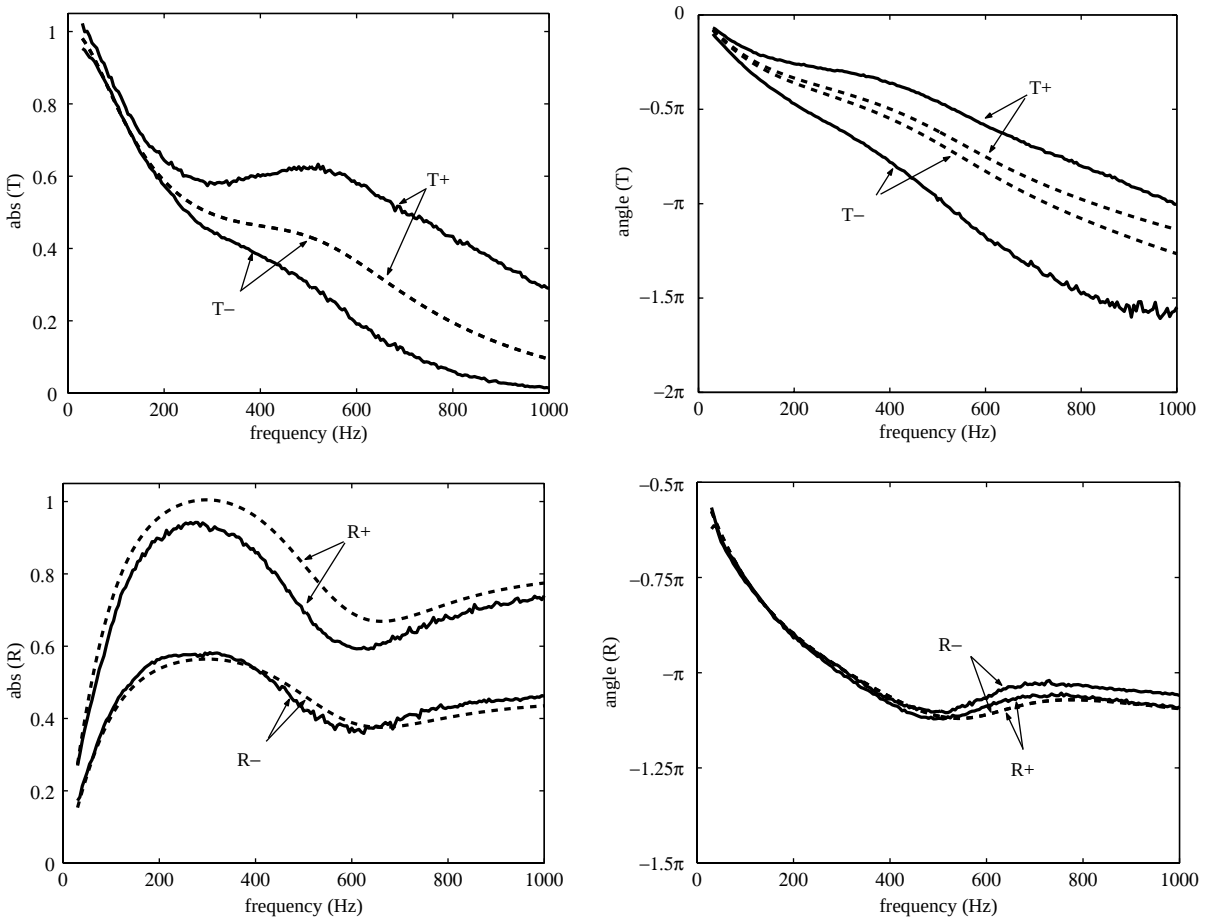

Fig. 6. Device 1: Comparison between the reflection and transmission coefficients measured for $M = 0.143$ (——) and predicted with the lumped model defined by equation (10) (– – –).

predicts the same absolute value of the transmission coefficient with and against the flow. In the experimental results, they are quite different: for example, the transmission coefficient with the flow T^+ is about 20 times as great as the transmission coefficient against the flow T^- at 1000 Hz for a Mach number $M = 0.143$. In the same way, the curves giving the angle of T are much farther apart in the experimental results than in the theory, in which only the effects of the convection along the chamber are taken into account. Similar results are observed for all devices described in Table 1.

There are two main assumptions in the segmentation model used. The first assumption states that the system can be considered as periodic; some couplings between the cells with flow can break the periodicity. The second assumption states that the lumped model is given by Eqs. (8) and (9). This model oversimplifies the complex interactions between the sound and the flow in the shear layer over the perforations. These assumptions are tested in the following sections.

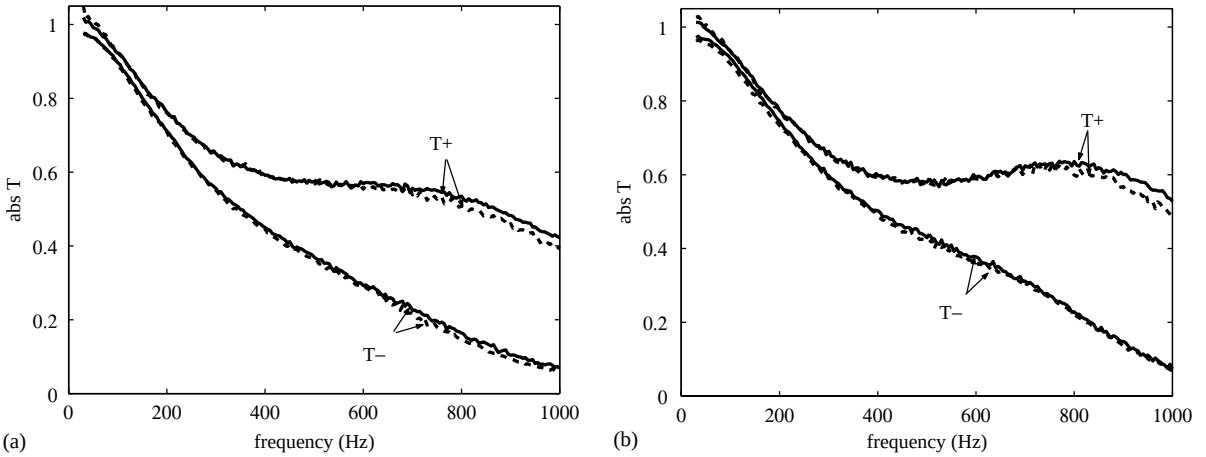

Fig. 7. Comparison of T measured for devices with 10 cells (——) and of T deduced from devices with 6 cells (– – –) ($M = 0.143$). (a), devices 1 and 2; (b), devices 3 and 4.

3.2. Independence of cell

The independence of the cells can be tested by computing the transfer matrix of one cell from two devices which only differ by the number of cells. If the system is periodic the two results are identical.

In Table 1, it can be seen that devices 1 and 2, and devices 3 and 4 only differ by the number of cells. Thus,

$$[\mathbf{T}_{c1}] = [\mathbf{T}]^{1/10}_{device\ 1} = [\mathbf{T}]^{1/6}_{device\ 2} \quad \text{and} \quad [\mathbf{T}_{c2}] = [\mathbf{T}]^{1/10}_{device\ 3} = [\mathbf{T}]^{1/6}_{device\ 4}. \tag{11}$$

Fig. 7 shows the Transmission coefficients T_p and T_m of devices 1 and 3 measured for $M = 0.143$, and deduced from the transfer matrices of one cell of devices 2 and 4, respectively. The results for devices 1 and 2, and for devices 3 and 4 are, respectively, very close. Similar results can be found for the other coefficients whatever the Mach number. Thus the assumption of independence of the cells is realistic.

3.3. Momentum conservation

In the perforation region, one could assume that there is no dissipation inside the region D (Fig. 5). This assumption leads to the conservation of the acoustical exergy $p + Mu$ [16] across the row of perforations. This assumption is the basis of Sullivan's theory [5] and leads to Eq. (8). One could as an alternative assume that there is no transfer of axial momentum through the perforations. This assumption leads to the conservation of $p + 2Mu$ across the row of perforations.

To determine which of the two assumptions is the most realistic, the scattering coefficients of the perforations row deduced from the matrix $[\mathbf{T}_p]$ are used. The value $(T_p^+ - 1)/R_p^+$ is equal to $(1 - M)/(1 + M)$ if the conservation of the exergy is applied and is equal to $(1 - 2M)/(1 + 2M)$ if the conservation of the axial momentum is applied. In the same way, $(T_p^- - 1)/R_p^-$ can be equal to

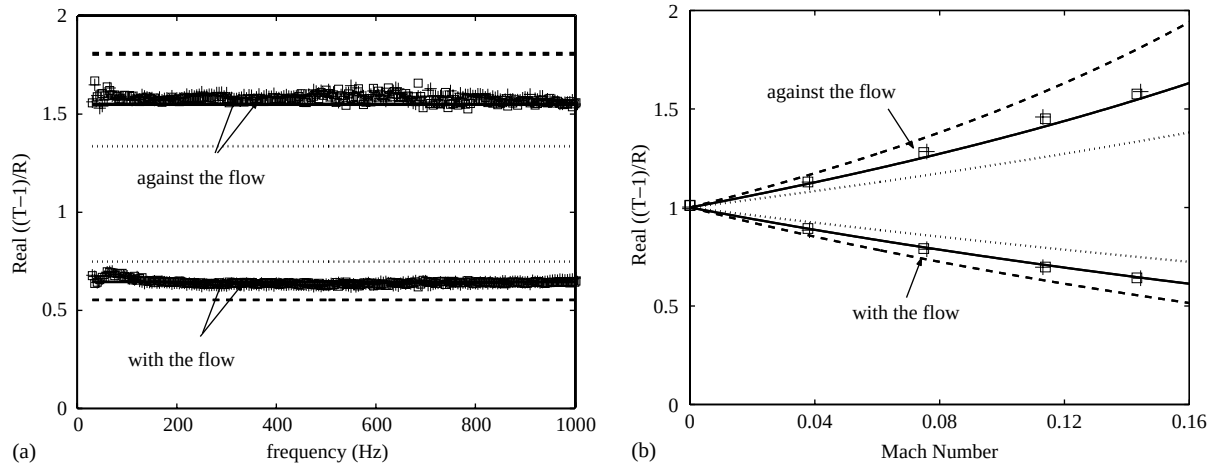

Fig. 8. Evolution of $real((T_p-1)/R_p)$ for $M=0.143$ as a function of the frequency (a), and of the Mach number (b). □, device 1; + + +, device 3. ——, $(1\pm1.5M)/(1\mp1.5M)$; – – –, $(1\pm2M)/(1\mp2M)$; ⋯, $(1\pm M)/(1\mp M)$.

$(1+M)/(1-M)$ (conservation of the exergy) or to $(1+2M)/(1-2M)$ (conservation of the axial momentum). The value $(T_p^{\pm}-1)/R_p^{\pm}$ is experimentally found to be a real number. Fig. 8a (devices 1 and 3) shows that this value is independent of the frequency at a given Mach number. Fig. 8b depicts the variation of this value as a function of the Mach number. The best fit of the experimental value is obtained by considering that

$$\frac{T_p^{\pm}-1}{R_p^{\pm}}=\frac{1\mp1.5M}{1\pm1.5M}.$$

This means that none of the above assumptions can be considered as valid.

Then equation (8) has to be replaced by

$$p_d+1.5Mu_d=p_c+1.5Mu_c. \tag{12}$$

3.4. Mass conservation

A close examination of the experimental data shows that the coefficient D_p is equal to 1, whatever the device and the Mach number. Thus, relating velocity on both sides of the perforations row leads to:

$$u_d=u_c+C_pp_c. \tag{13}$$

It is surprising that this empirical equation is the same as the equation without flow. Together with Eq. (12), this equation implies that the best fit of the transfer matrix of a perforations row is

$$\begin{pmatrix}p_d\\u_d\end{pmatrix}=\begin{bmatrix}1-1.5MC_p & 0\\ C_p & 1\end{bmatrix}\begin{pmatrix}p_c\\u_c\end{pmatrix}. \tag{14}$$

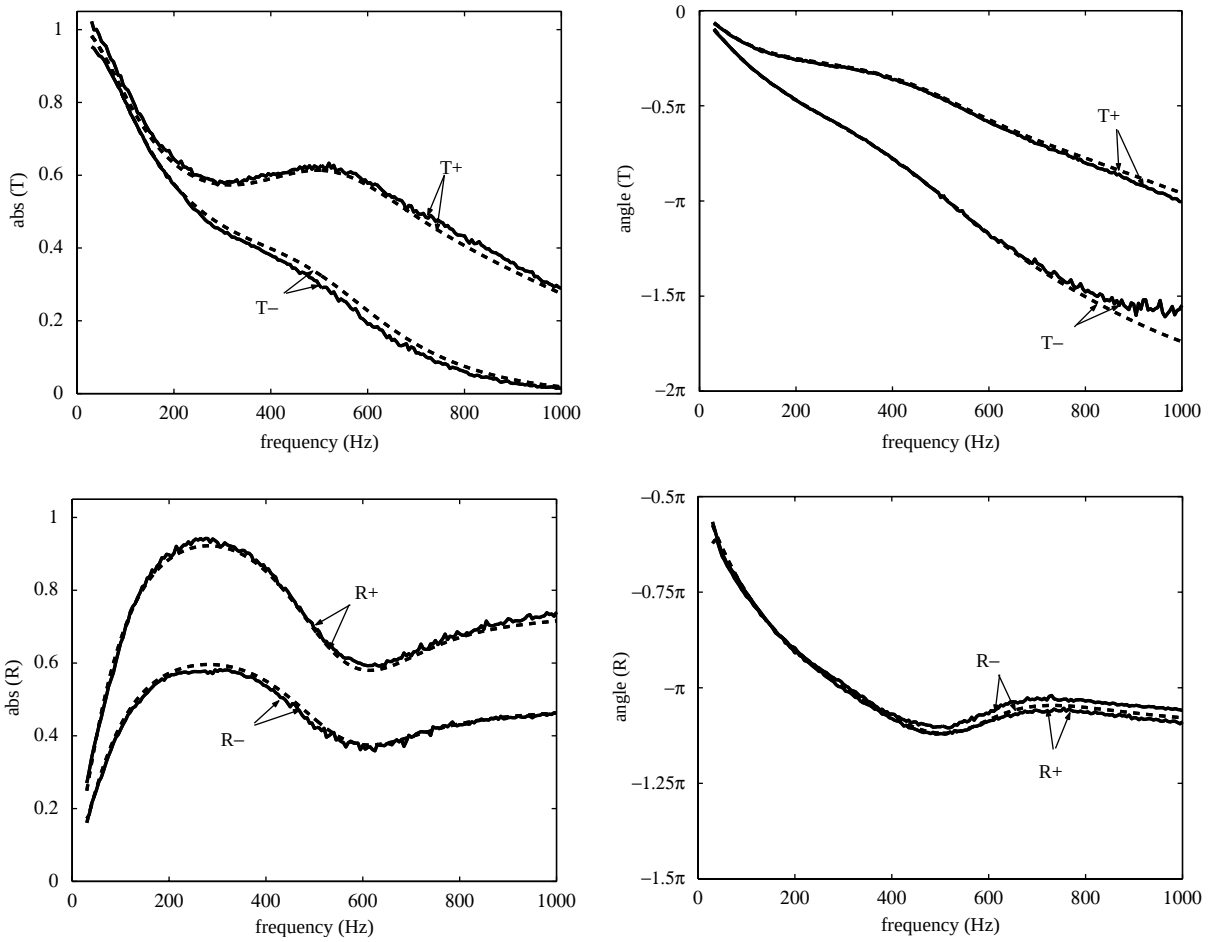

Fig. 9. Device 1: comparison between the reflection and transmission coefficients measured for $M = 0.143$ (——), and predicted with the lumped model defined by equation (14) (– – –).

The coefficient C_p is linked to the admittance of the perforations plus the back cavity. By mass conservation in the region D (Fig. 5), the velocity v_p going through the perforations is equal to

$$v_p = \frac{S_t}{S_p}(u_c + Mp_c - (u_d + Mp_d)) = \frac{-S_t C_p(1 - 1.5M^2)}{S_p} p_c, \tag{15}$$

where S_t and S_p are the areas of the perforated tube and of the row of perforations. Then, the coefficient C_p is proportional to the admittance of the perforations plus the back cavity defined by $Y_c = v_p/p_c$. It could be noted that this definition of the admittance is not the only one. The admittance can also be defined by $Y_c = v_p/p_d$ which leads to a different value.

In the same way as in Section 3.1, the scattering coefficients of the partitioned chamber with a perforated tube are calculated using Eqs. (14), (5) and (6). These coefficients are compared in Fig. 9 to the measured value for device 1. The agreement is good. Thus a segmentation method

can be used to make a model of the acoustical behaviour of a perforated tube if a correct lumped model is used.

4. Conclusion

Experiments were performed at low frequencies on a perforated tube with a partitioned chamber. Four different configurations were studied and the results lead to a revision of the classical segmentation model. The assumption of independence of the cells is validated by the experimental results. The classical lumped model of Sullivan [5] based on the conservation of exergy of the flow through the perforations does not agree with the experimental data. The assumption that there is no axial momentum transfer to the wall, as a result of the flow through the perforations, also fails to explain the experimental results. An empirical model which fits the data is proposed.

The assumptions of exergy conservation and axial momentum conservation fail to explain the experimental results. Some momentum is transferred into the perforations and some energy is lost. A similar behaviour was found in the continuous description of lined wall with flow. The classical condition is the continuity of the acoustic radial displacement at the wall [17]. It was experimentally demonstrated that a more realistic condition is between displacement and velocity continuities [18]. This new condition can be explained by considering the effect of the viscosity in the acoustic and hydrodynamic boundary layers [19]. One of the effects of viscosity is to transfer some momentum from the main flow to the wall. The same type of effect seems to appear here. Thus, it could be worthwhile to analyze the effect of flow on the acoustical behaviour of a perforation in a viscous fluid.

References

[1] K.S. Peat, A numerical decoupling analysis of perforated pipe silencer elements, Journal of Sound and Vibration 123 (1988) 199–212.
[2] E. Dokumaci, Matrizant approach to acoustic analysis of perforated multiple pipe mufflers carrying mean flow, Journal of Sound and Vibration 191 (1996) 505–518.
[3] P.O.A.L. Davies, M.F. Harrison, H.J. Collins, Acoustic modelling of multipath silencers with experimental validations, Journal of Sound and Vibration 200 (1997) 195–225.
[4] A.H. Nayfeh, J.E. Kaiser, D.P. Telionis, Acoustics of aircraft engine-duct systems, American Institute of Aeronautics and Astronautics Journal 13 (1975) 130–153.
[5] J.W. Sullivan, A method for modelling perforated tube muffler components, i. theory, Journal of Acoustic Society of America 66 (1979) 772–778.
[6] J. Kergomard, A. Khettabi, X. Mouton, Propagation of acoustic waves in two waveguides coupled by perforations, i. theory, Acta Acustica 2 (1994) 1–16.
[7] M. Pachebat, J. Kergomard, Interferences of two propagating modes at low frequencies in ducts coupled by periodic perforations, Comptes Rendus de l'Académie des Sciences, Series IIB 326 (1998) 881–886.
[8] G. Brzózka, Acoustic filters with two perforated tubes, Archives of Acoustics 16 (1991) 461–474.
[9] E. Dokumaci, A discrete approach for analysis of sound transmission in pipes coupled with compact communicating devices, Journal of Sound and Vibration 239 (2001) 679–693 (doi:10.1006/jsvi.2000.3126).
[10] M. Åbom, Measurement of the scattering-matrix of acoustical two-port, Mechanical System and Signal Processing 5 (1991) 89–104.

[11] G. Ajello, Mesures acoustiques dans les guides d'ondes en présence d'écoulement: mise au point d'un banc de mesure, application à des discontinuités, Ph.D. Thesis, Université du Maine, Le Mans.
[12] D. Ronneberger, Genaue Messung der Schalldampfung und der Phasengeschwindigkeit in durch stromten Rohren im Hinblick auf die Wechselwirkung zwischen Schall und Turbulenz, Habilitation thesis, Universität Göttingen, Göttingen.
[13] D. Ronneberger, C.D. Ahrens, Wall shear stress caused by small amplitude perturbations of turbulent boundary-layer flow: an experimental investigation, Journal of Fluid Mechanics 83 (1977) 433–464.
[14] M.C.A.M. Peters, A. Hirschberg, A.J. Reijnen, A.P.J. Wijnands, Damping and reflection coefficient measurements for an open pipe at low mach and low helmholtz numbers, Journal of Fluid Mechanics 256 (1993) 499–534.
[15] M.S. Howe, The damping of sound by wall turbulent shear layers, Journal of Acoustical Society of America 98 (1995) 1723–1730.
[16] R. Starobinski, Y. Aurégan, Fluctuations of vorticity and entropy as sources of fluctuating exergy, Journal of Sound and Vibration 216 (1998) 521–527.
[17] M.K. Myers, On the acoustic boundary condition in presence of flow, Journal of Sound and Vibration 71 (1980) 429–434.
[18] Y. Aurégan, M. Leroux, Experimental investigation of the wall condition in lined ducts with flow, Presented at the 5th CEAS-ASC Workshop on Turbomachinery Noise and Duct Acoustics, Eindhoven, 2001.
[19] Y. Aurégan, R. Starobinski, V. Pagneux, Influence of grazing flow and dissipation effects on the acoustic boundary conditions at a lined wall, Journal of Acoustical Society of America 109 (2001) 59–64 (doi: 10.1121/1.1331678).